

**UNIVERSITÀ DEGLI STUDI DEL PIEMONTE ORIENTALE
“AMEDEO AVOGADRO”**

DIPARTIMENTO DI SCIENZE DEL FARMACO

**Corso di Laurea Magistrale in Chimica e Tecnologie
Farmaceutiche**

TESI DI LAUREA

**Synthesis of sphingolipids analogs as potential dihydroceramide
desaturase (Des1) inhibitors**

**Relatore
Prof. Luigi Panza**

**Candidato
Claudio Sacchi**

**ANNO ACCADEMICO 2023-2024
Sessione autunnale**

Abbreviations

AcOEt: ethyl acetate

AcOH: acetic acid

ap: apparent

Boc: tert-butyloxycarbonyl

br: broad

Coa: coenzyme A

COSY: correlation spectroscopy

DCM: dichloromethane

Des: dihydroceramide desaturase

Dhceramide: dihydroceramide

d: doublet

dd: doublet of doublets

dt: doublet of triplets

EDC: 1-ethyl-3-(3-dimethylaminopropyl)carbodiimide

eq: equivalents

GDT: global distance test

Glu: glutamic acid

h: hours

His: histidine

HMBC: heteronuclear multiple bond correlation

HMPA: hexamethylphosphoramide

HOBt: hydroxybenzotriazole

HRMS: high-resolution mass spectrometry

HSQC: heteronuclear single quantum coherence spectroscopy

IC50: half minimal inhibitory concentration

IQAC-CSIC: Institut de Química Avançada de Catalunya – Consejo Superior de Investigaciones Científicas

IR: infrared

J: coupling constant

Ki: inhibitory constant

m: multiplet

MeOH: methanol

min: minutes

m.p.: melting point

p: pentuplet

q: quadruplet

r.t.: room temperature

s: singlet

t: triplet

td: triplet of doublets

THF: tetrahydrofuran

TMSCF₃: trimethyl(trifluoromethyl)silane

Tyr: tyrosine

Table of Contents

Abstract	1
Introduction	2
Biosynthesis of Ceramide and Des1 action	3
Known Des1 Inhibitors	4
Previously performed SINTCARB group work	6
Computational approach and Alphafold 2	7
Objectives of the work	14
Results and discussion	15
Synthetic approach	15
Synthesis of aminodiol	15
Functionalization with carboxylic acids	21
Biological evaluation of product 6 and 7	21
Conclusion and future work	23
Experimental section	24
General methods	24
Bibliography and citations	34
Sitography	38

Abstract

Balance in levels of ceramide has been linked to control of cell survival, and as such biochemical paths to its production arose as interesting new targets for drug design. Among these enzymes, dihydroceramide desaturase 1 (Des1) represents a desirable point of interaction, catalyzing a simple transformation that happens as the last step of the de-novo synthesis of ceramide. At the same time, targeting Des1 presents complications derived by the absence of crystallized structure of said enzyme or its homologues. Nevertheless, structures capable of inhibiting this target have been synthesized in the past, although drug activity rationale is not clear.

This master's thesis will focus on the synthesis of N-acyl modified analogues of previously synthesized PR280 inhibitor, in order to unveil how changes in the structure of this portion of the molecule can impact the biological activity of this derivatives. Moreover, the larger scope of this work is the structural rationalization of drug-enzyme interaction to obtain more potent inhibitors for Des1. Synthesis of hexanamide and decanamide bearing analogues was successful through a six-step synthesis with an overall yield of 16.4% and 14.7%, respectively.

In addition to work performed in SINTCARB laboratories under professor Maribel Matheu (Universidad Rovira et Virgili, Tarragona), this work couldn't be carried out without the respective contribute given by docking studies in collaboration with professor Xavier Barril (University of Barcelona) laboratory and biological evaluation done by professor Gemma Fabriàs laboratory (IQAC-CSIC, Barcelona).

Introduction

“Sphingolipids are found in all animals, plants, and fungi, and in some prokaryotic organisms and viruses. They are composed of a sphingoid base backbone to which a fatty acid may be attached through an amide bond and a head group at the primary hydroxyl”¹. This family of molecules has a key role in the transduction of signals and in cell regulation, with a higher relevance in neurons². Lately they have been recognized as having a role in the apoptosis/cell survival axis, and as such studied as a suitable druggable target in pharmaceutical studies³.

One of such biological pathways can be described as an interconversion between sphingosine bioactive derivatives, also known as the sphingosine rheostat balance. This observation, first proposed in 1996⁴, states that the pro-apoptotic and growth-stopping signal given by ceramide⁵ (via the TNF α pathway) and the cell survival promotion resulting from sphingosine-1-phosphate signaling⁶ are linked via the enzymatic transformation of the common substrate sphingosine.

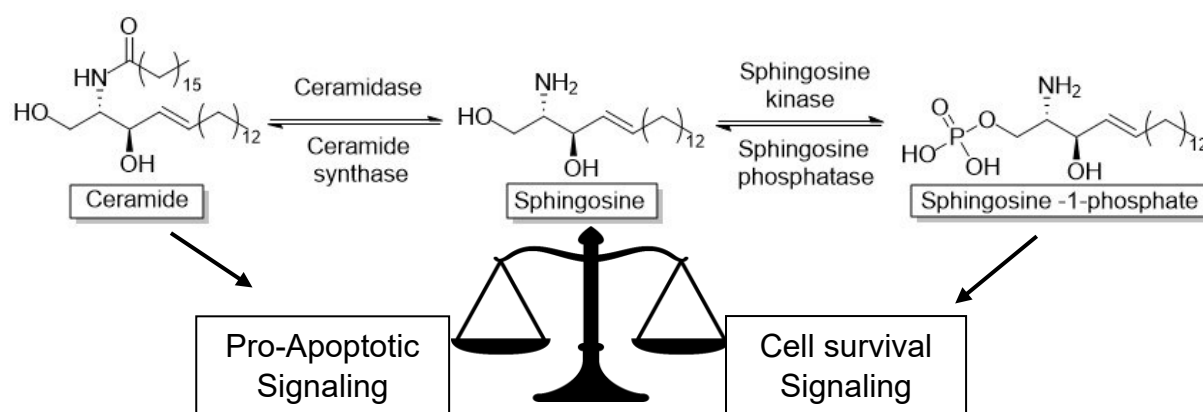


Figure 1: Visual representation of sphingosine rheostat balance

¹ A. H. Merrill, *Biochemistry of Lipids, Lipoproteins and Membranes* (Fifth Edition); Elsevier, 363-397 (2008).

² M. Lee, S.Y. Lee, Y.S. Bae; Functional roles of sphingolipids in immunity and their implication in disease. *Exp Mol Med* **55**, 1110–1130 (2023).

³ S. Grassi, L. Mauri, S. Prioni, L. Cabitta, S. Sonnino, A. Prinetti, P. Giussani; Sphingosine 1-phosphate receptors and metabolic enzymes as druggable targets for brain diseases; *Frontiers in Pharmacology*, **10**, 807 (2019).

⁴ O. Cu villier, G. Pirianov, B. Kleuser, P.G. Vanek, O.A. Coso, J.S. Gutkind, S. Spiegel, Suppression of ceramide-mediated programmed cell death by sphingosine-1-phosphate; *Nature*, **381** (6585), 800-803 (1996).

⁵ L.M. Obeid, C.M. Linardic, L.A. Karolak, Y.A. Hannun; Programmed Cell Death Induced by Ceramide. *Science*, **259** (5102), 1769–1771 (1993).

⁶ S. Pyne, D.R. Adams, N.J. Pyne, Sphingosine 1-phosphate and sphingosine kinases in health and disease: Recent advances; *Progress in Lipid research*, **62**, 93-106 (2016).

Biosynthesis of Ceramide and Des1 action

In vivo there are the two main pathways to produce ceramide: the de novo synthesis and the degradation of sphingomyelin, but it seems that the two differently generated ceramides have separate roles in cell regulation, though the relation between this ceramides pool are not clear⁷. The de novo path takes place in the Golgi apparatus and starts with a reaction between serine and palmitoyl-Coa mediated by serine palmitoyl transferase. Then, the newly formed aminoketone gets reduced to alcohol by 3-Ketosphinganine reductase, forming dihydrosphingosine. Said molecule has to be acylated by dihydroceramide synthase, getting to the key intermediate dihydroceramide. In the end ceramide is formed by the Δ -4 desaturase action of dihydroceramide desaturase. This enzyme has two allosteric forms: a ubiquitary form named Des1, which will have a central point within the discussion of this thesis, and Des2, a form that presents C-4 hydroxylase activity and can produce other molecules (phytoceramides)⁸. Des2 is mainly present in skin and intestine, and as a less explored molecule will not be part of this work.

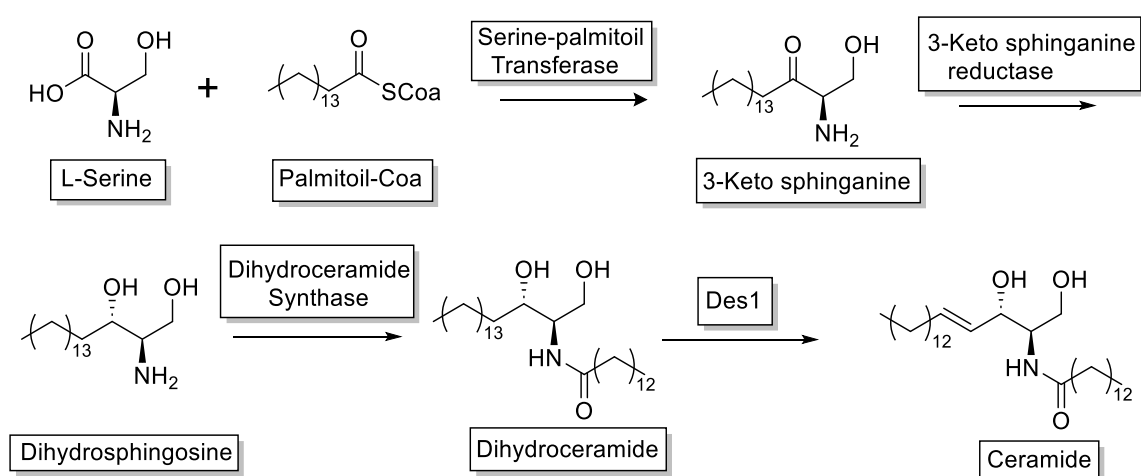


Figure 2: The novo synthesis of ceramide

In 2006, Merrill et al observed during a treatment of human prostate cell with fenretinide (4-hydroxyphenylretinamide) that those cells presented high

⁷ C.P. Reynolds, B.J. Maurer, R.N. Kolesnick; Ceramide synthesis and metabolism as a target for cancer therapy, *Cancer Letters*, 206 (2), 169-180 (2004).

⁸ M.M. Siddique, Y. Li, B. Chaurasia, V.A. Kaddai, S.A. Summers; Dihydroceramides: From bit Players to Lead Actors, *Journal of Biological Chemistry*, 290 (25), 15371-15379 (2015).

concentration of dihydroceramide and unexpectedly low amounts of ceramide⁹. These results suggested that dhceramide, at the time considered a non-bioactive intermediate, could instead be responsible for the antitumoral effect of fenretinide and led the group to explore how control of the sphingosine rheostat balance influenced this equilibrium. This difference in biological action can likely be attributed to the difference in polarity between ceramides and dhceramides, that inhibits the later species ability to cross bilayer membranes¹⁰.

Starting from those considerations Des1 can become a target in drug design in order to control the sphingosine rheostat. In particular dihydroceramide could influence oxidative stress regulation, hypoxia, autophagy induction, inflammation and proliferation¹¹, whilst also being profiled for the treatment of diseases such as cancer, diabetes, and even treatment of AIDS¹².

Known Des1 Inhibitors

Finding inhibitors for Des1 is a challenging task, since not only there has not been any recording of the crystallized structure, but even analog structures are absent from the PUBMED databases. The most potent inhibitor of Des1 to date was described by Llebaria et al in 2001 His name is GT11 and it consist in a C8-cyclopropenil ceramide, working as a competitive dose-dependent inhibitor of Des1 ($K_i = 6 \mu M$, $IC_{50} = 23 nM$) with activity expressed both in vitro and in live cells. Although the crystallized structure is still unknown, the supposed way of function of the molecule was by a reaction between a free cysteine side chain in the enzyme and the cyclopropene ring of the compound¹³.

⁹ W. Zheng, J. Kollmeyer, H. Symolon, A. Momin, E. Munter, E. Wang, S. Kelly, J.C. Allegood, Y. Liu, O. Peng, H. Ramaraju, M. Cameron Sullards, M. Cabot, A.H. Merrill; Ceramides and other bioactive sphingolipid backbones in health and disease: Lipidomic analysis, metabolism and roles in membrane structure, dynamics, signaling and autophagy; *Biochimica et Biophysica Acta (BBA) – Biomembranes*, 1758 (12), 1864-1884 (2006).

¹⁰ F.X. Conteras, G. Basañes, A. Alonso, A. Hermann, F.M. Goñi; Asymmetric addition of ceramides but not dihydroceramides Promotes transbilayer (Flip-Flop) Lipid Motion in Membranes, *Biophysical Journal*, 88(1), 348-359 (2005).

¹¹ S. Rodriguez-Cuenca, N. Barbarroja, A. Vidal-Puig; Dihydroceramide desaturase 1, the gatekeeper of ceramide induced lipotoxicity, *Biochimica et Biophysica Acta (BBA) – Molecular and Cell Biology of Lipids* 1851 (1), 40-50 (2015).

¹² A. Ashkenazi, M. Viard, L. Unger, R. Blumenthal, Y. Shai; Sphingopeptides: dihydrosphingosine-based fusion against wild-type and enfuvirtide-resistant HIV-1, *FASEB Journal*, 26 (11), 4628 (2012).

¹³ G. Triola, G. Fabriàs, A. Llebaria; Synthesis of a Cyclopropene Analogue of Ceramide, a Potent Inhibitor of Dihydroceramide Desaturase. *Angewandte Chemie (International ed. In English)*, 40 (10), 1960-1962 (2001).

Using analogues of GT11 we can map which are the most important sites of the molecule in order to retain the biological effect:

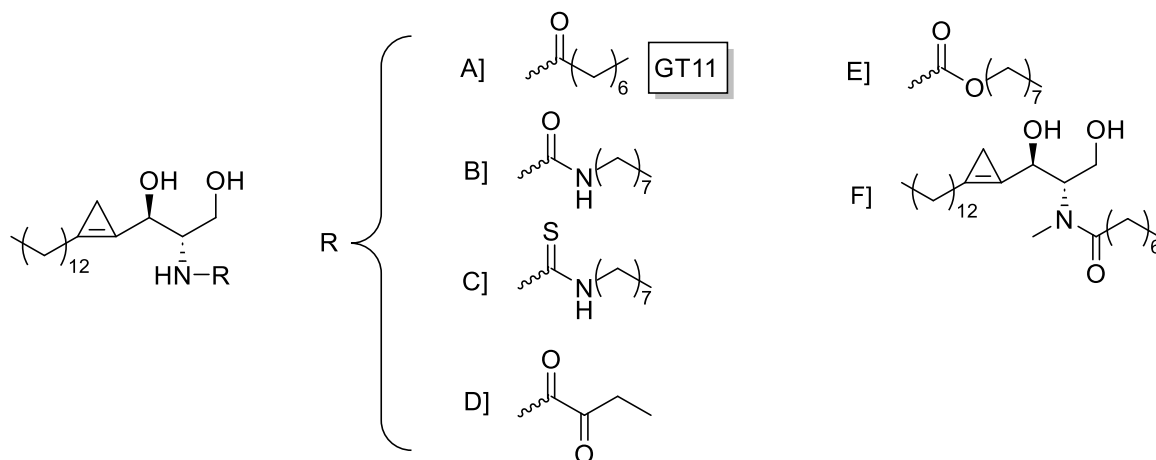


Figure 3: GT11 derivatives

- N-acyl modifications: by substituting the amide moiety with a urea (B), thiourea (C) or an α -keto-amide (D) the compound retains the activity (although with lower potency), while methylation of the amide nitrogen (F) or the substitution with a carbamate (E) make the derivate lose inhibitory effect¹⁴.
- N-acyl chain length: only *N*-hexanoyl (6) and *N*-decanoyl (10) derivatives retained the inhibitory effect, although at lower potencies ($IC_{50}=31 \mu M$ for hexanoic acid derivate, $13 \mu M$ for decanoic acid). The supposed explanation of this phenomenon is interchange in cell permeability¹³.
- Cyclopropene modifications: GT11 cyclopropenone structure is not the only one reported to maintain inhibitory activity. The perfect example for this is XM462 and its derivatives, where the cyclopropene has been removed and at its place a sulfur atom is placed in the main chain in position 5. This compound has excellent biological properties ($IC_{50}=8.2 \mu M$ in vitro and $0.78 \mu M$ in vivo, both in a dose dependent manner)¹⁵, and can also induce autophagy in HG27 human gastric cancer cell line. Other analogues of

¹⁴ C. Bedia, G. Triola, J. Casas, A. Llebaria, G. Fabriàs; Analogs of the dihydroceramide desaturase inhibitor GT11 modified at the amide function: synthesis and biological activities; *Organic & Biomolecular Chemistry*, 3 (20), 3707-3712 (2005).

¹⁵ J.M. Munoz-Olaya, X. Matabosh, C Bedia, M. Egido-Gabás, J. Casas, A. Llebaria, A. Delgado, G. Fabriàs; Synthesis and biological activity of a novel inhibitor of dihydroceramide desaturase; *ChemMedChem: Chemistry Enabling Drug Discovery*, 3 (6), 946-953 (2008).

XM462 are also active in Des1 inhibition, but with less potency, probably derived from the polarity difference given by the absence of C3 hydroxyl group¹⁶.

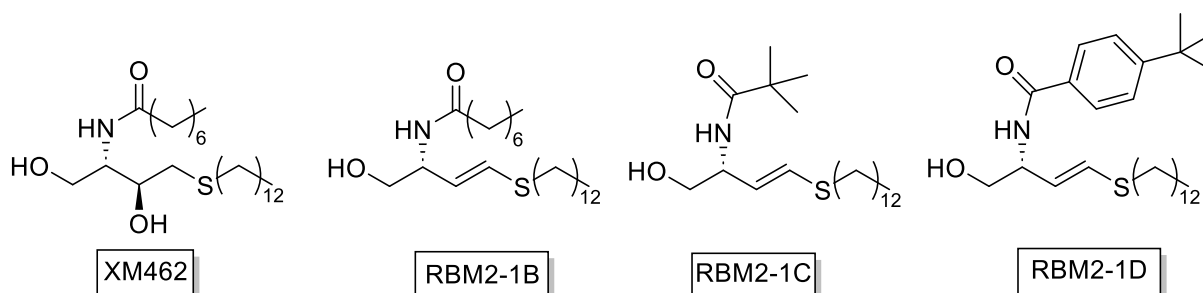


Figure 4: XM462 derivatives

Previously performed SINTCARB group work

The first step towards the design of new active structures directed to act on Des1 is to rationalize the activity of previously discovered compounds, and to do so the group started a study comparing active molecules of various structure to identify the molecular motifs that could maximize interaction.

The requirements found were:

- A 2S, 3R aminoalcohol *anti* moiety;
- A C1 free hydroxyl substituent;
- A secondary amide structure in 2.

By using these data as a baseline, the group then explored different solutions to expand the pool of molecules that could possess those parameters.

One of the first way to apply those teachings was the introduction of different triazole groups (1,4 disubstituted 1,2,3 triazole¹⁷ or 1,5 disubstituted 1,2,3 triazole¹⁸) (**S1**, **S2**). These structures can be used as an isostere thanks to both their ability to

¹⁶ L. Camacho, F. Simbari, M. Garrido, J.L. Abad, J. Casas, A. Delgado, G. Fabriàs; 3-Deoxy-3,4-dehydro analogs of XM462. Preparation and activity on sphingolipid metabolism and cell fate; *Bioorganic & Medicinal Chemistry*, 20 (10), 3173-3179 (2012).

¹⁷C. Martí Torrell; Synthesis of potential dihydroceramide desaturase 1 inhibitors based on triazole motifs as a therapeutic target against cancer; Master thesis, Universitat Rovira i Virgili, SINTCARB group (2018).

¹⁸ P. Rivero Prieto, PhD student, SINTCARB group.

mimic the conformational impairment caused by the cyclopropenone ring and the rigidity added to the structure, whilst also maintaining the ability to form π - π stacking interactions^{19,20}. Moreover, the newly added triazole group could have the benefit to form dipole-dipole bonds, given the two new sites in form of the nitrogen atoms. Unfortunately, this kind of structures while showing inhibitory activity in intact cells (up to 30%), did not show any in cell lysates.

Another class of molecule explored were compounds in which the cyclopropenone ring was substituted with 1-4 disubstituted furan (**S3**)¹⁸. As for the triazole derivatives, this kind of choice was made by looking at the heterocyclic center as an isostere for the cyclopropenone ring maintaining the same characteristics (π - π stacking bond and the ability to accept hydrogen bonds). In addition the furan ring can oxidize, and it was thought this structure could possibly increase chelation to the enzyme²¹. This furan based derivatives reached 45% of inhibition.

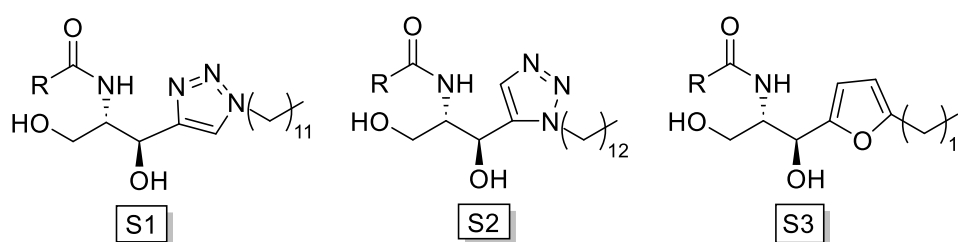


Figure 5: Illustration of previously synthesized Des1 Inhibitors in the SINTCARB group

Computational approach and Alphafold 2

The main difficulty in those initial approaches was that they were done in absence of any type of structural information in regards of the targeted enzyme. In fact, to

¹⁹ E. Bonandi, M.S. Christodoulou, G. Fumagalli, D. Perdicchia, G. Rastelli, D. Passarella; The 1,2,3-triazole ring as a bioisostere in medicinal chemistry, *Drug Discovery Today* 22 (10), 1572-1581 (2017).

²⁰ G. Appendino, S. Bacchiega, A. Minassi, M.G. Cascio, L. DE Petrocellis, V. Di Marzo; The 1,2,3-Triazole Ring as a peptido- and olefinomimetic element: discovery of click vanilloids and cannabinoids, *Angewandte Chem* 119 (48), 9472 (2007).

²¹ L.A. Peterson; Reactive Metabolites in the Biotransformation of Molecules Containing a Furan Ring; *Chemical Research in Toxicology*, 26 (1), 6-25 (2013).

this day crystallized Des1 structures are not available, meaning that we had to base our structure designs on uncertain parameters.

AlphaFold 2 is an open-source software that, using the aminoacidic composition of a protein, is able to generate a prediction of his tridimensional structure with a high interval of probability (92.4 GDT out of 100, correspondent to 1.6 Å error, evaluated using the Global Distance Test). It was developed by DeepMind and EMBL-EBI (European Bioinformatic Institute, part of the European Molecular Biology Laboratory family) and it is based on an artificial intelligence that has at his disposal 170000 structures^{22,23}. On July 21 of 2021, AlphaFold 2 released a high-quality prediction of the structure of the entire human proteasome, in a work that was sure to spark interest in the academic community. Among other, there finally was a confident depiction of Des1, that could finally bolster the research of new derivatives²⁴.

In light of the insight collected from this research, a collaboration with Dr. Xavier Barril of University of Barcelona was initiated with the aim of elucidating the Des1 properties and identifying potential novel ways for enzyme inhibition. In specific, Dr. Barril team found a believable position to introduce the prosthetic non eme di-oxo Fe group, necessary for the abstraction of hydrogen and the overall function of the molecule. The theorized site was located in a lipophilic pocket, where the prosthetic group could be stabilized by bounds between Iron atoms and lateral chains: one Fe atom would be coordinated to five histidine residues (His89, His93, His128, His132 and His262), while the other metallic atom by four histidine residues and one glutamic acid (His131, His233, His263, His259 and Glu232).

²² J. Jumper et al; AlphaFold 2. Fourteenth Critical Assessment of Techniques for Protein Structure Prediction (2020).

²³ L.M. Bertoline, A.N. Lima, J.E. Krieger, S.K. Teixeira; Before and after AlphaFold2: An overview of protein structure prediction; *Frontiers in Bioinformatics*, 3, 1120370 (2013).

²⁴ AlphaFold 2 Protein Structures Database, <https://alphafold.ebi.ac.uk/entry/O15121>.

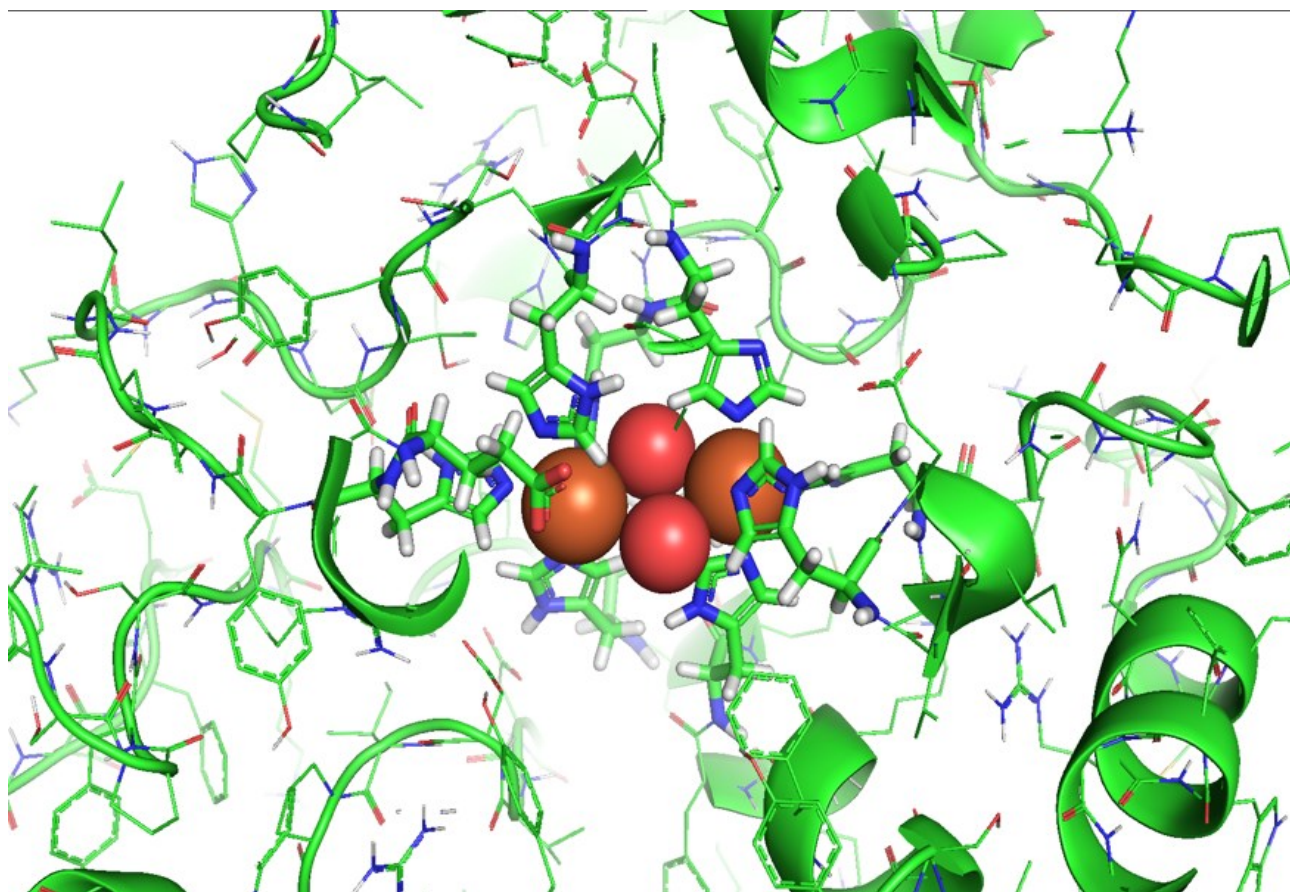


Figure 6: Supposed position of the Fe₂O₂ prosthetic group

Using this newly constructed active site and once again in collaboration with Professor Xavier Barril's team, docking studies were commenced, utilizing as reference GT11 and XM462, the two most powerful inhibitors known to that point. This would be a highly effective way to simulate the relative position that these molecules would assume, and from those spatial data extrapolate further criteria to construct new molecules (preferred conformations, formation of secondary binding sites...).

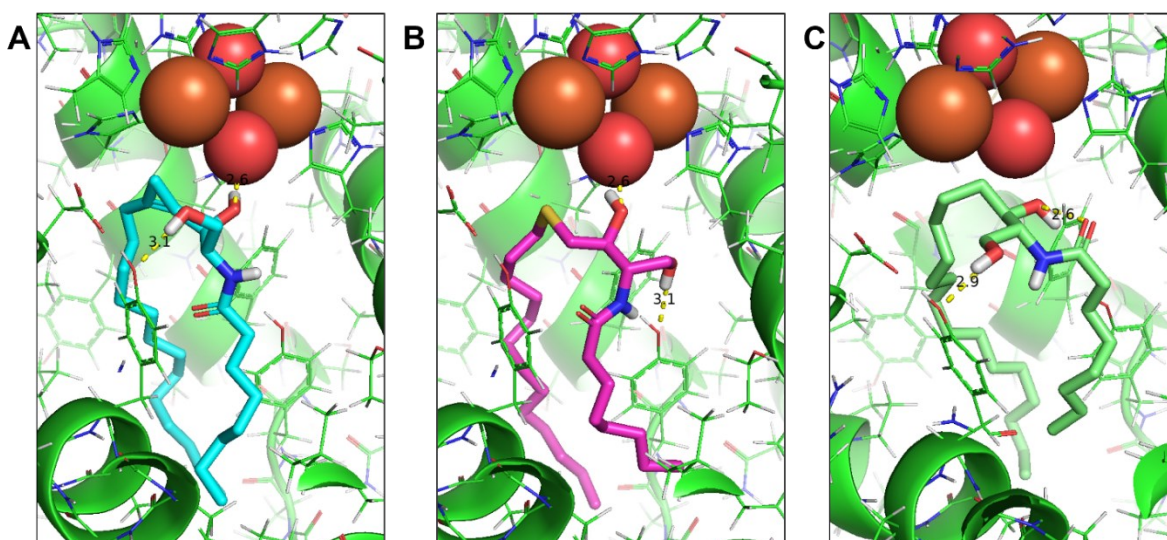


Figure 7: Docking conformation comparison between Dihydroceramide (C), GT11 (A) and XM462 (B) inside Des1 active site.

As it is seen in figure 7A of GT11, the conformation that achieved the best docking scores presents the acyclic chains bifolded and the cyclopropene ring in the proximity of one of the iron atoms. Moreover, the position of the bound C3 hydroxyl moiety suggests the formation of a hydrogen bond with an oxygen of the prosthetic group, while the C1 hydroxyl forms a hydrogen bond with an aminoacidic residue of the pocket (Tyr170). Furthermore, GT11 supposed way of inhibition of the enzyme has been debunked. In fact, it was thought that the cyclopropene ring would form a covalent bond with a free cysteine residue¹³, while such residues are absent from the active site.

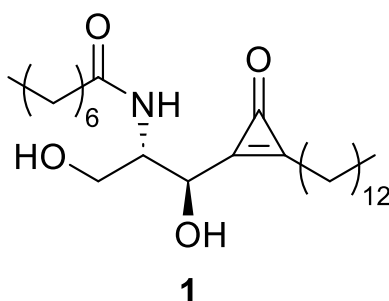
XM462 (figure 7B) adopts a similar bifolded shape, with the same hydrogen bond between the C3-hydroxyl group and the oxygen atom, while the sulfur atom participates in an interaction with the iron atom of the cluster. The C1-hydroxyl forms a bond with Tyr120 rather than Tyr170.

Previously synthesized products from the group were also evaluated in these docking studies. The majority of the structures does not assume the bifolded conformation, and by doing so the interaction of hydroxyl residues with the active site is compromised, possibly leading to loss or reduction of activity.

Using these newfound observations, we could update the theoretical requirements that a novel structure directed to inhibit Des1 should possess:

- The molecule should adopt a bifolded conformation in the active site;
- C4 and/or C5 position in the active site should be proximal to one of the Iron atoms of the Fe₂O₂ group;
- OH-3 should interact with one of the oxygen atoms of the prosthetic group;
- OH-1 should perform a hydrogen bond, acting as a donor, with a residue outside the active site;
- Any drug-design aimed at obtaining irreversible cysteine binding should be discarded, due to the absence of said residue near the active site of the enzyme.

Subsequently, the group tried exploring this chemical space with new molecules. One proposed way of action was the substitution of the cyclopropene ring of GT11 with a cyclopropenone. This kind of structure can be advantageous in several different ways: the cyclopropenone ring can undergo 1,2- and 1,4- addition reaction, both referred as suitable to achieve inhibition on proteins²⁵. Furthermore, the carbonyl group could theoretically interact with the prosthetic group, leading to a stronger interaction and a favorable geometry. The structure is also stable in biological solvents, as it is already present in commercially available molecules²⁶.



To verify those assumptions, a docking study was done in collaboration with Xavier Barril group. According to these results, the binding mode with the highest score sees OH-1 forming a hydrogen bond with Glu232 and OH-3 bound through another hydrogen bond to one of the oxygen atoms of the prosthetic group, while the

²⁵ J. Sasa, H. Zhangxu, D. Yuanbing, J. Gang, W. Kaiyue, Y. Feifei, Z. Jingyu; An Overview of cyclopropanone derivate as promising bioactive molecules, *Bioorganic & Medicinal Chemistry Letters*, 129845 (2024).

²⁶ H. Tokuyama, M. Isaka, E. Nakamura, R. Ando, Y. Morinaka; Synthesis and biological activities of cyclopropanone antibiotic penitricin and congeners, *The Journal of antibiotics*, 45 (7), 1148-1154 (1992).

position of the carbonylic portion is compatible with the coordination of one iron atom to Fe_2O_2 .

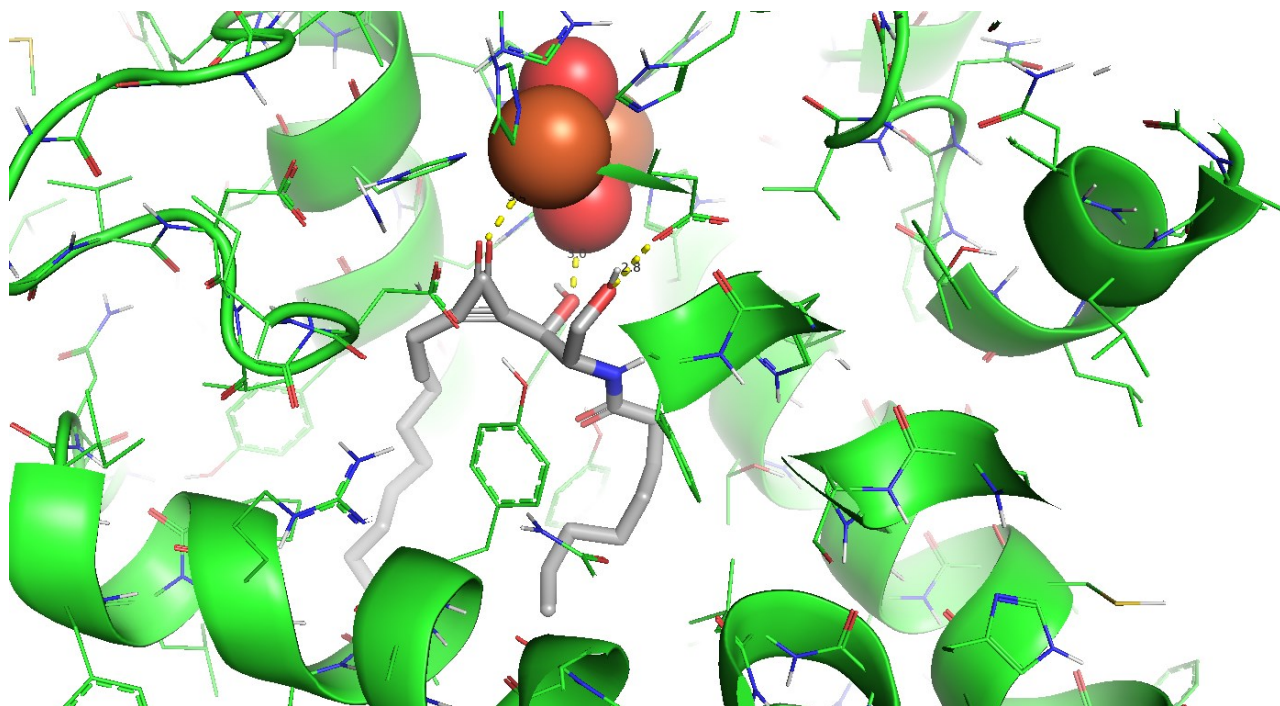


Figure 8: PR280 conformation in active site of Des1

Assured by this data, the group decided to synthesize the compound, which was achieved through a 6 step synthesis starting from 1-pentadecyne (the approach that will be further discussed in the results and discussion section) under the name of PR280.

The molecule was then promptly evaluated in biological studies in collaboration with the group led by Prof. Gemma Fabriàs (IQAC-CSIC, Barcelona). The data from these tests were very promising, with a better inhibition activity than XM462 in both in vitro and in vivo experiments ($\text{IC}_{50}=0.7 \mu\text{M}$ in cell lysates). This excellent activity is plausible and confirms how the interactions in the docking studies are related to strong biological activities.

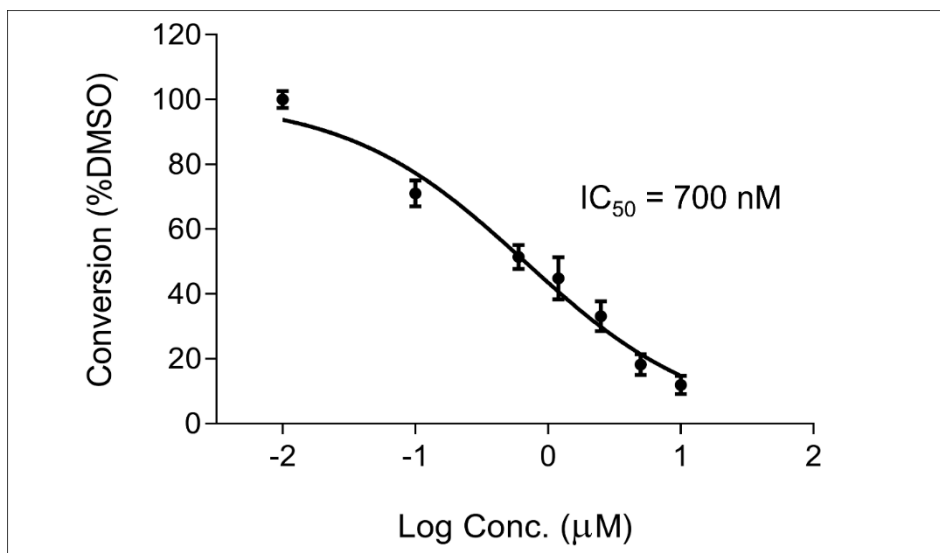


Figure 9: Concentration-dependence curve for PR280 in T98 cells

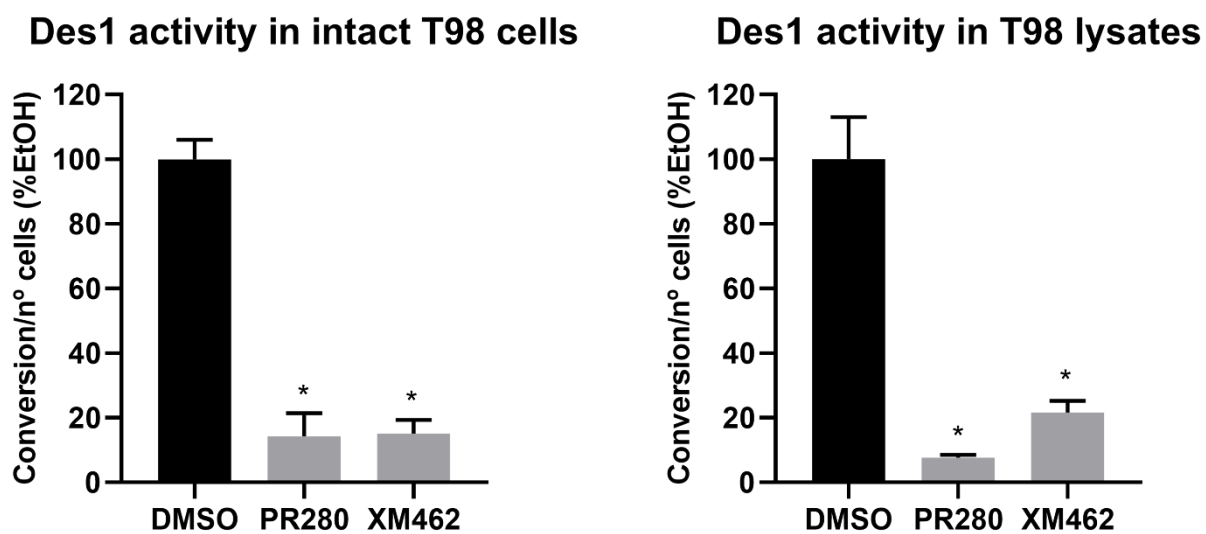


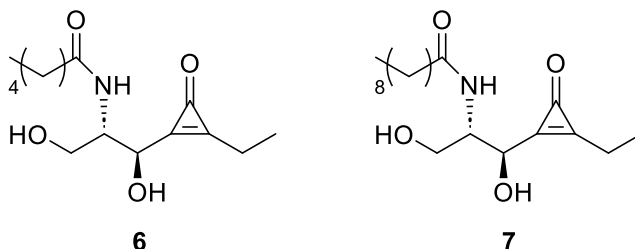
Figure 10: Confrontation of effect between PR280 and XM462 effect in T98 cells

Objectives of the work

The primary objective of this master's thesis is the investigation, synthesis and biological evaluation of derivatives of PR280. In particular we will focus on modification of N-acyl structures with the goal to understand how these structural modifications impact the interaction between the synthesized derivatives and the target enzyme Des1 and find structures that enhance the activity.

By systematically altering the N-acyl groups of PR280, this research aims to construct a small library of modified cyclopropenone molecules, in order to shed light on secondary structural features that influence the binding affinity and enzymatic activity of Des1. This could lead to the construction of small molecules with higher inhibition and rationalize the way N-acyl chains modify structural activity relations.

In order to obtain active molecules and without previous parameters to follow from docking studies, we decided to indulge in a similar procedure as the one used in the exploration of GT11 derivatives. With this in mind, we chose to obtain PR280 analogues with modified linear N-acyl chain length following the best results obtained in GT11 structure/activity studies (6 C and 10 C)¹³. For this reason, the structures we aimed at synthesizing are amides **6** and **7**.



It is important to specify that at the time this thesis was getting worked on, the team was waiting for the results of a docking study that was being performed under Professor Xavier Barril's team (University of Barcelona) in order to screen the library of structures and have more consistent basis to identify new possible molecules. Unfortunately, the timing of those studies didn't allow these docking results to be used, so results of the latter will not be reported in the present thesis.

Results and discussion

Synthetic approach

Based on previous synthesis of PR280 done in the SINTCARB group, we decided that the best line of work would be to first synthesize aminodiol **5** as a common precursor and afterwards subject it to N-acylation with the correspondent carboxylic acid in order to obtain the final amide. This method permits great flexibility, being capable of storing product **5** and overall reduce the amount of work to obtain the desired products.

Synthesis of aminodiol **5**

Product **5** can be obtained by total deprotection of product **4**, who is the result of stereoselective addition of the lithium salt of product **3** to (S)-Garner's aldehyde. Said product can originate by the protection of cyclopropenone **2**, which itself can be generated starting from pentadecyne with a [2+1] cycloaddition followed by subsequent hydrolysis of product **1**.

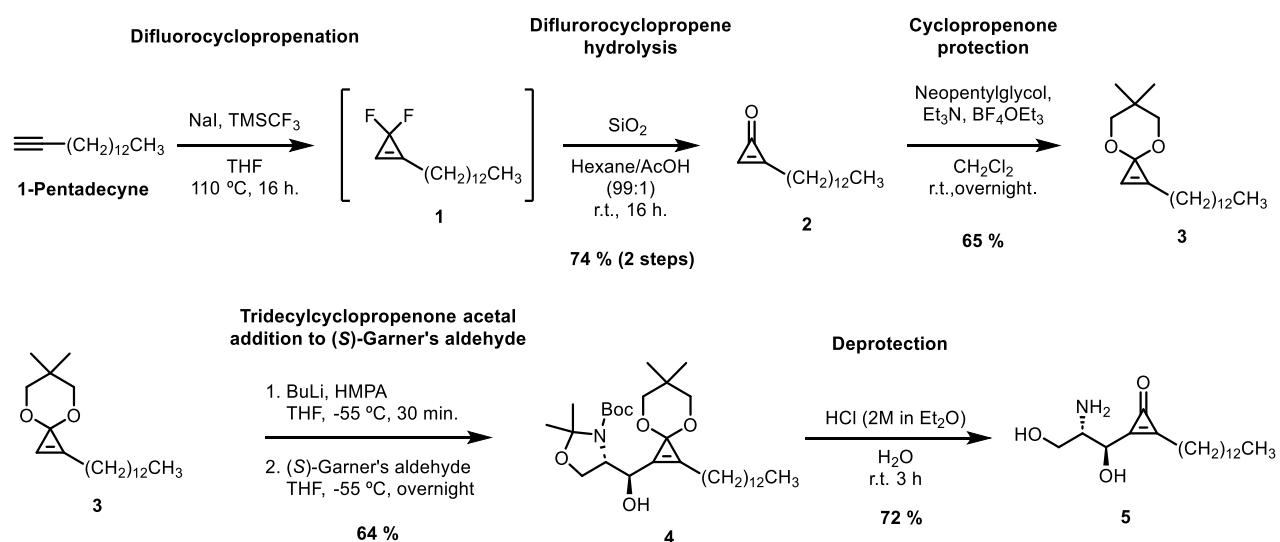


Figure 11: Complexive synthesis of aminodiol

It is crucial to highlight that the reactions up to the synthesis of aminodiol **5** have been extensively studied in the SINTCARB group and this overall synthesis is the result of numerous attempts and corrections. This explains the reason for why some of the choices for this specific synthetic route were made.

For example:

- [2+1] cycloaddition on the alkyne motif can only be performed previously to the addition to Garner's aldehyde, since the amine presence can negatively impact difluorocarbene reactivity in regards of the triple bond;
- The use of Garner's aldehyde towards the end of the synthesis allows to decrease the waste of this expensive reagent, introducing possible stereochemical problems later in the synthetic pathway.

The first synthetic step consists in the [2+1] cycloaddition reaction between 1-pentadecyne and difluorocarbene in order to obtain difluorocyclopropene **1**. The selected source of difluorocarbene is the commercially available Ruppert-Prakash reagent (TMSCF₃), which has been demonstrated to generate the reactive species when heated in presence of NaI²⁷.

From the addition product **1** the supposed reaction progression would follow the spontaneous release of one F atom as an anion, forming an aromatic fluorocyclopropen cation intermediate, that afterwards reacts with a water molecule. Cyclopropenone would then be obtained by the spontaneous elimination of HF, that in our reaction was neutralized in the work up process using NaHCO₃²⁸.

²⁷ F. Wang, T. Luo, J. Hu, Y. Wang, H.S. Krishnan, P.V. Jog, S.K. Ganesh, G.K. Surya Prakash, G.A. Olah; Synthesis of *gem*-Difluorinated Cyclopropanes and Cyclopropenes: Trifluoromethyltrimethylsilane as a Difluorocarbene Source, *Angewandte Chemie International Edition*, 50 (31), 7153-7157 (2011).

²⁸ Z.-L. Cheng, Q.-Y. Chen; Difluorocarbene Chemistry: A Simple Transformation of 3,3-*gem*-Difluorocyclopropenes to Cyclopropenones, *Chinese Journal of Chemistry*, 24 (9), 1219-1224 (2006).

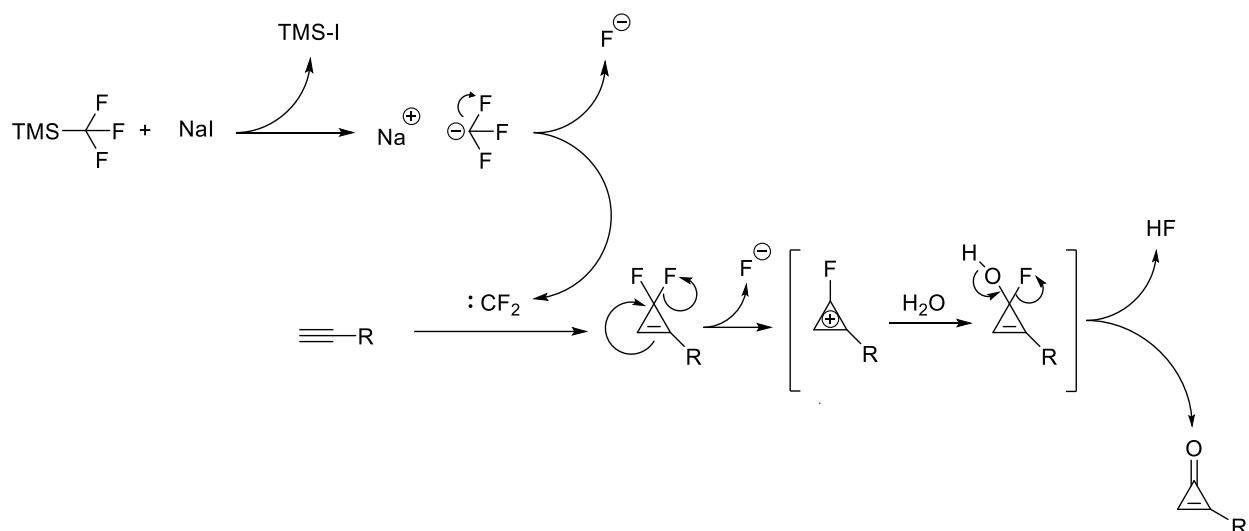


Figure 12: Supposed mechanism of cyclopropenone **2** synthesis

The reaction was carried out in a closed tube at high temperature (110°) using 5 equivalents of TMSCF₃ and an excess amount of NaI (2 equivalents), using THF as a solvent, as it gives higher yields in comparison with DME and acetonitrile (74% overall yield on the two step reaction).

Difluorocyclopropene intermediates naturally tend to hydrolyze forming cyclopropenone, so proton NMR must be done rather quickly and it is not possible to characterize them by ¹³C. Alternatively, the presence of unreacted intermediate **1** could be detected by using Fluorine NMR techniques.

The presence of a carbonylic moiety in the molecule is incompatible with the addition to Garner's aldehyde due to the strong basic reaction conditions. For this reason, the sensitive ketone was protected using neopentylglycole, giving the correspondent acetal. This type of reaction is rather unusual, since cyclopropenone protected acetals are usually generated in situ via base catalyzed dehydrohalogenative cyclization of acetals²⁹.

²⁹ M. Nakamura, I. Hiroyuki, E. Nakamura; Cyclopropenone acetals synthesis and reactions, Chemical reviews, 103 (4), 1295-1326 (2003).

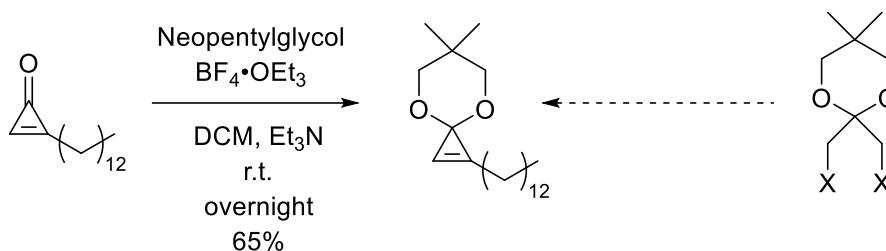


Figure 13: Protection of cyclopropenone

Protected cyclopropenone **3** can now be used in the key addition to (S)-Garner's aldehyde ((S)-(-)-3-Boc-2,2-dimethyloxazolidine-4-carboxaldehyde)³⁰. This previously nominated reagent is a versatile building block to introduce in our compound a 2-amino-1,3-dihydroxypropyl motif, which is a structure found in many biologically active molecules³¹.

Additionally, proper reaction conditions give the product as a sole diastereomer³². The selectivity of this type of alpha-amino-alcohol addition is often explained in bibliography via the contraposition of two models: the Felkin-Anh transition state and the Cram chelate state³³.

Following the Felkin-Anh model, the Newman projection would put the NBoc group in a perpendicular position with respect to the carbonyl group, due to the favorable $n-\pi^*$ interaction possible in this position with carbonyl oxygen lone pair of electrons. The nucleophile then attacks from the least sterically hindered side following the Bürgi-Dunitz trajectory, giving the *anti*-product (Figure 14, **A**).

Formation of *syn*-product is instead explained following Cram's chelate model. In this case, presence of a metal atom such as Mg^{+2} , Zn^{+2} , Cu^{+2} , Ti^{+4} , Ce^{+3} or Mn^{+2} can coordinate both the carbonyl and the N-protected group. The consequence for the formation of this chelate is an eclipsed Newmann's projection. In this situation

³⁰ P. Garner, J.M. Park; The synthesis and configurational stability of differentially protected .beta.-hydroxy-.alpha.-amino aldehydes, *The Journal of Organic Chemistry*, 52 (12), 2361-2364 (1987).

³¹ X. Liang, J. Andersch, M. Bols; Garner's aldehyde, *Journal of Chemical Society, Perkin Transactions 1*, (18), 2136-2157 (2001).

³² M. Passiniemi, A.M. Koskinen; Garner's aldehyde as a versatile intermediate in the synthesis of enantiopure natural products, *Beilstein journal of organic chemistry*, 9 (1), 2641-2659 (2013).

³³ O.K. Karjalainen, A.M. Koskinen; Diastereoselective synthesis of vicinal amino alcohols, *Organic & Biomolecular Chemistry*, 10 (22), 4311-4326 (2012).

the nucleophile is free to attack from a perpendicular angle to the carbonyl, always from the least hindered side (Figure 14, **B**).

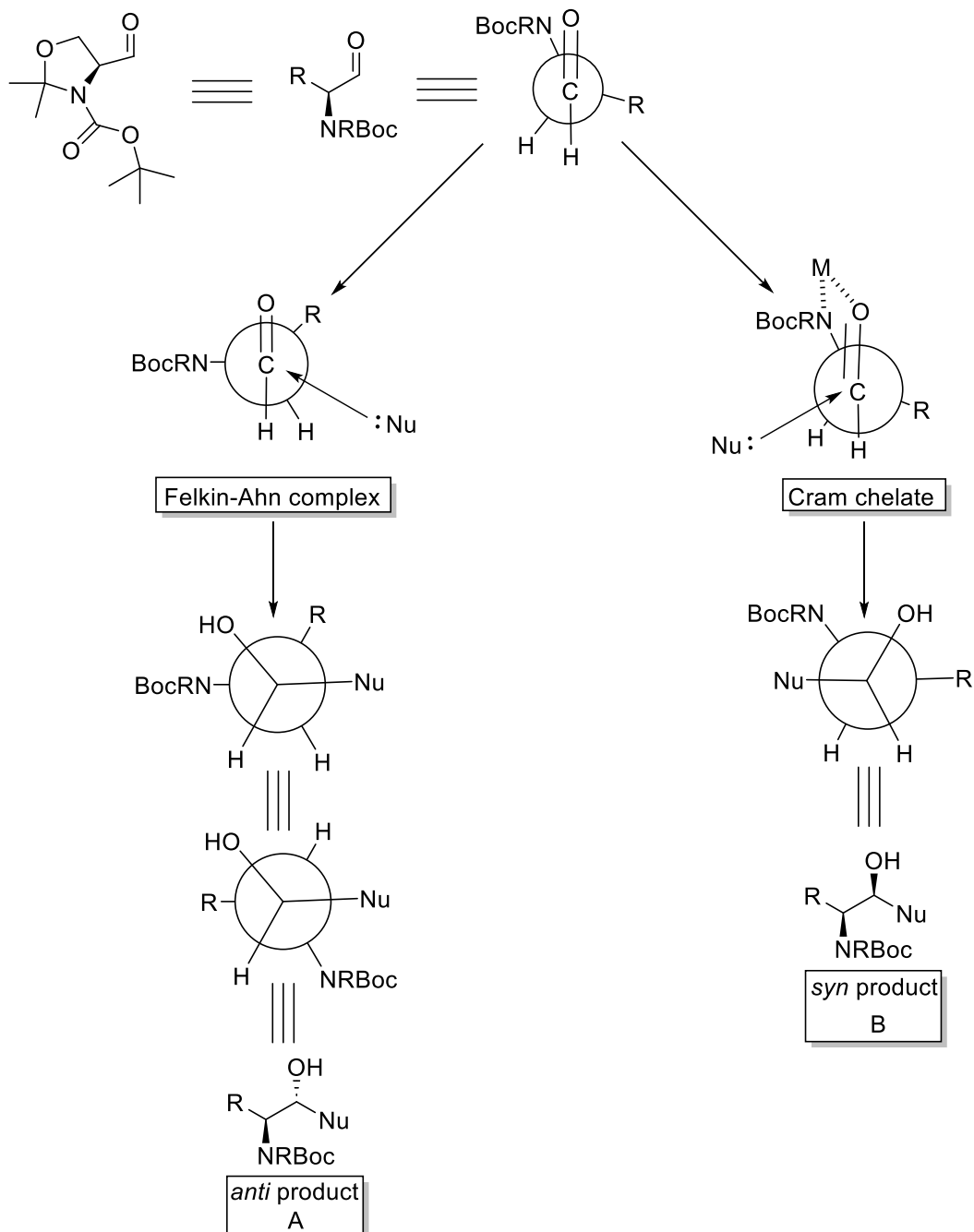


Figure 14: Visualization of Garner's aldehyde addition stereoselectivity

Since we strove to obtain the *anti*-product, we worked in absence of any possible chelating metals, so following the Felkin-Ahn model. Furthermore other conditions can be manipulated to maximize the formation of *anti*-diastereomer:

- Reaction temperature is a key parameter for the formation of *anti*-diastereomer. In fact, if the addition is carried at -15 C°, a *syn*-*anti* mixture is obtained, while working at lower temperatures favors formation of *anti*-product³⁴. This happens because the activation bearing to the desired *anti* product is lower than the one for correspondent *syn* diastereoisomer, thus kinetic control is favorable;
- The formation of a Li⁺ cluster can limit the nucleophilicity of the cyclopropenonyl anion, disfavoring the addition. To balance this problematic HMPA was added as an effective way to coordinate the cations and break the Li⁺ cluster³⁵.

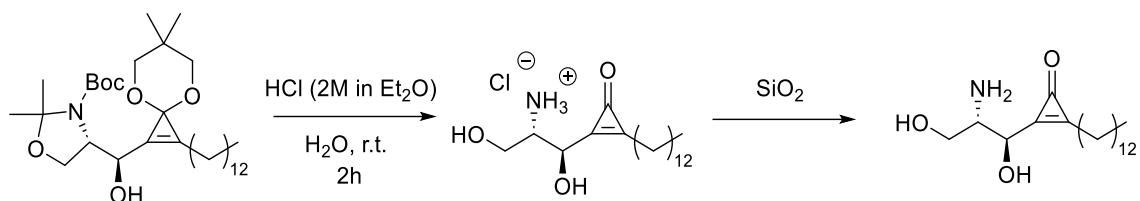
Purification of product **4** was complicated by the presence in the product of various impurities, one among all unreacted Garner's aldehyde, that possess the same retention factor of the researched molecule. This problematic is reflected in a less than expected yield (64%).

Additionally, ¹H NMR analysis of this product is complicated by his nature, since it is composed by a couple of rotamers, making deciphering the spectra's data difficult. For a better understanding we recorded the spectra at different temperatures: at lower temperatures the different conformers appear as two separate entities due to the slower interconversion speed, while at higher T the result is an average of the single isomers values.

Product **4** was ultimately deprotected using a large excess of HCl in aqueous solution, giving the correspondent salt on the nitrogen atom. Said salt was deprotonated to amine by means of flash column chromatography with neutralized silica gel. We must note that obtaining the free aminodiol was a relevant improvement, as a problem previously encountered in the group, was that the salt cannot be subjected to N-acylation and was difficult to convert it to free amine¹⁸.

³⁴ L. Wong, S. Tan, Y. Lam, A.J. Melendez; Synthesis and evaluation of sphingosine analogues as inhibitors of sphingosine kinases, *Journal of Medicinal Chemistry*, 52 (12), 3618-3626 (2009).

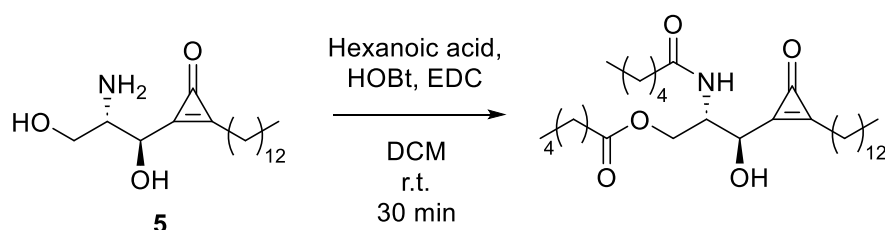
³⁵ W.H. Sikorski, H.J. Reich; The regioselectivity of addition of organolithium reagents to enones and enals: the role of HMPA, *Journal of the American Chemical Society*, 123 (27), 6527-6535 (2001).



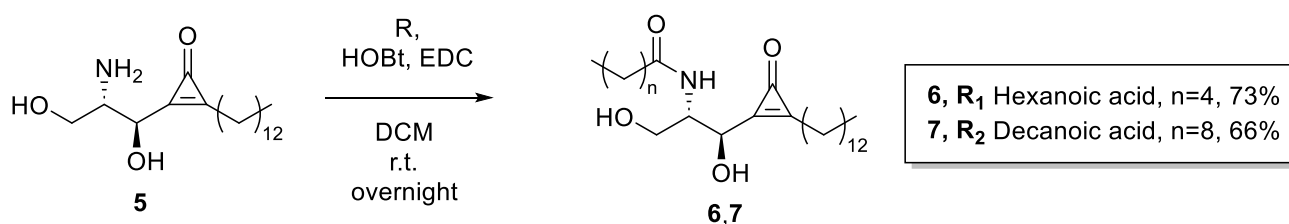
Functionalization with carboxylic acids

The N-acylation was done using hydrobenzotriazole (HOBt) and 1-Ethyl-3-(3-dimethylaminopropyl)carbodiimide (EDC) as coupling agents, as well as both hexanoic acid and decanoic acid.

Unfortunately, the first reaction resulted in the multiple aspecific acylation between the desired ammine and C1-OH. Moreover, attempts to recover the desired product through Zemplén deacetylation reaction were unsuccessful.



Thankfully by diminishing the amount of starting reagents (1.1 eq of carboxylic acid, EDC and HOBt compared to the 1.8 eq of the three used in previous attempts) the unwanted esterification could be prevented.



In this way both products were obtained through a total number of 6 steps, with a total yield of 16.4 % for product **6** and 14.8% for product **7**.

Biological evaluation of product 6 and 7

During the time this thesis was being written, the larger scope of this project was the obtainment of a library of structures bearing the **5** aminodiol base structure with different N-acyl lateral chains to evaluate through a computational approach. With

this set of PR280 related molecule in hand we could then start a larger docking study, comparing how different side chain interact with Des1. The highest scoring molecules could then be easily synthesized in the SINTCARB lab via N-acylation starting from the stored aminodiol **5**.

The synthesized new molecules would then be tested in biological essays under Professor Gemma Fabriàs Laboratories (IQAC-CSIC, Barcelona). Unfortunately, as already reported results for this library weren't available until the end of practical work.

Since some time has passed from the end of this thesis work, the SINTCARB group published an article³⁶ including the results of this thesis work in the overall synthesis of PR280 and his derivatives. Sadly from the information reported in this study, PR280 remains the most powerful among synthesized Des1 inhibitors.

³⁶ P. Rivero, V. Ivanova, X. Barril, M. Casampere, J. Casas, G. Fabriàs, Y. Díaz, M.I. Matheu; Targeting dihydroceramide desaturase 1 (Des1): Syntheses of ceramide analogues with a rigid scaffold, inhibitory assays, and AlphaFold2-assisted structural insights reveal cyclopropanone PR280 as a potent inhibitor, *Bioorganic Chemistry*, 145, 107233 (2024).

Conclusion and future work

From the work done we can abstract the following conclusions:

- The synthesis of PR280 analogues **6** and **7** has been successful following the proposed approach of a six step synthesis, with respective overall yields of 16,4% (**6**) and 14,76% (**7**);
- Product **6** and **7** will be tested for biological activity under Professor G. Fabriàs group;
- We have achieved a rather fast way to obtain N-acylated PR280 derivatives;
- Deprotection of **4** has given higher yields than previous iteration in the SINTCARB group.

In conclusion, sphingosine and his derivatives continue to obtain high interest in the research of bioactive compounds, and it is easy to see the reason. The field is ever expanding as we find more applications in medicinal chemistry for this class of molecules, and as the horizon of possible uses for those molecules broadens, at the same way the synthetic routes become more accurate.

Future work will focus on the synthesis of best scoring molecules indicated by docking studies results in collaboration with Xavier Barril team, in order to obtain more powerful molecules able to exert their inhibitory activity on Des1.

Experimental section

Clarifications

Since collected structures until aminodiol 5 were already synthesized in previous works in the SINTCARB group, full characterization of product is only reported for newly obtained molecules **6**, **7** and PR280. In the course of the synthesis other products were only identified by H¹ and C¹³ NMR.

We report data from the highest obtained yield for each reaction.

General methods

All reactions sensible to atmospheric conditions were conducted in anhydrous conditions using Argon gas; any glass equipment required in these reactions was first dried in heated stove and then subjected to Argon-vacuum cycles. When adding solvents or reagents to the reaction mixture we used syringes previously subjected to the same cycles.

Instrumentation

- IR spectra were obtained with a JASCO FT/IR-680 plus infrared spectrophotometer and visualized with SpectraManager software (JASCO®);
- All NMR data (¹H, ¹³C, COSY, HSQC, HMBC) are obtained with a Varian Mercury VX 400 and analyzed with MestreNova software (MestreLab®);
- Melting points (M.p.) were obtained with a Mettler Toledo DSC 822°;
- High-resolution mass spectra (HRMS) were obtained using an Agilent 1100 Series LC/MSD mass spectrometer with electrospray ionization (m/z values are expressed in Dalton);
- Optical rotations α_D^{25} were obtained with a Perkin-Elmer 241 polarimeter with a path length of 1.0 dm;
- Thin layer chromatography was performed using 0.25 mm E.Merck® silica plates (60 F₂₅₄ silica);
- Flash column chromatography was conducted using Fluka® and Merk® silica gel 60.

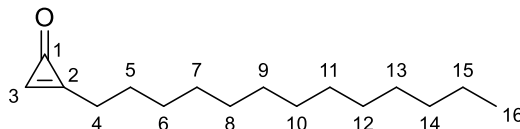
All waste was collected and disposed under SINTCARB procedures.

NMR coupling constants are expressed in Hz and their description follows the following abbreviations:

- s = singlet;
- d = doublet;
- t = triplet;
- q = quadruplet;
- p = pentuplet;
- m = multiplet;
- dd = doublet of doublets;
- dt = doublet of triplets;
- td = triplet of doublets;
- ap = apparent;
- br = broad.

Numerations of the following molecules may differ from IUPAC norms, since it is based of sphingosine chemistry.

2-tridecycycloprop-2-en-1-one Synthesis (product 1)



In a Schlenk tube 1-pentadecyne (2 mL, 7.62 mmol) and NaI (2.5135 g, 16.77 mmol) were weighted and then dissolved in dry THF (10.2 mL) under a positive Argon pressure. At this point TMSCF_3 (5.63 ml, 38.09 mmol) was added, the system was isolated and put at 110 C° under vigorous stirring overnight.

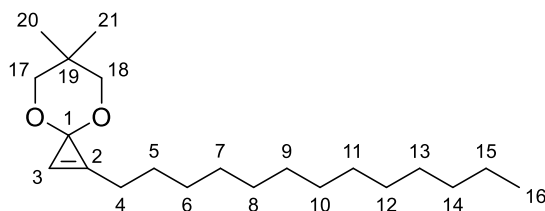
After 20 hours the reaction was quenched by addition of a saturated solution of NaHCO_3 under stirring. The resulting phases were separated and the aqueous phase was extracted using Et_2O . The combined organic phases were dried using Na_2SO_4 , filtered and concentrated under vacuum. The crude presents itself as a brown oil.

The crude was dissolved in 140 mL of hexane / acetic acid (99:1) silica gel was added, and the mixture was left stirring overnight at room temperature. After the reaction end the crude was filtered under vacuum and washed several times with hexane and AcOEt. Afterwards a NaHCO_3 saturated solution was added under stirring, and then subsequent washes with a NaHCO_3 saturated solution were performed, followed by an extraction using both hexane and AcOEt. The collected organic phases were dried using Na_2SO_4 and concentrated under vacuum. The product presents itself as a yellow-brownish oil. Said oil was purified via flash column chromatography on silica gel, using as a mobile phase a solution hexane/AcOEt (7:3→6:4) and concentrated under vacuum, giving a white solid (1.3396 g, 74.4 % yield).

^1H NMR (400 MHz, solvent CDCl_3) δ in ppm: 8.42 (s, 1H, H3), 2.68 (t, J = 7.3 HZ, 2H, H4), 1.72 (q, J = 7.3 Hz, 2H, H5), 1.445-1.345 (m, 2H, H6), 1.332-1.26 (m, 20H, from H7 to H15), 0.88 (t, J = 10.3 Hz, 3H, H16). **^{13}C NMR** (100.6 MHz, CDCl_3) δ in ppm: 170.3 (C-2), 158.0 (C-1), 148.2 (C-3), 32.0 (CH_2), 29.70 (CH_2), 29.68

(2CH₂), 29.6 (CH₂), 29.5 (CH₂), 29.4 (CH₂), 29.2 (CH₂), 29.0 (C-6), 27.5 (C-4), 25.7 (C-5), 22.7 (CH₂), 14.2 (C-16).

6,6-dimethyl-1-tridecyl-4,8-dioxaspiro[2.5]octi-1-ene Synthesis (product 2)



In a round bottom flask product **1** (1.3396 g, 5.66 mmol) and BF₄OEt₃ (1.6044 g, 8.49 mmol) were added, then dissolved with dry DCM (9,3 mL) under positive Argon pressure and left stirring for 30 minutes at room temperature. In another round bottom flask neopentylglycole (1.214 g, 11.66 mmol) and dry triethylamine (1.57 mL) were dissolved in dry DCM (3 mL) under positive argon pressure and at room temperature. After the 30 minute checkmark the neopentylglycole solution was added dropwise in 30 minute and the resulting mixture was left stirring at room temperature overnight.

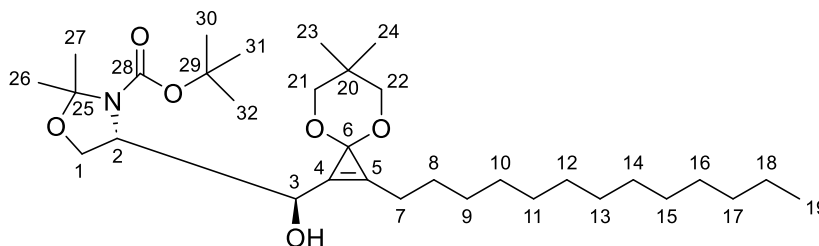
The resulting reaction crude was quenched by adding a NaHCO₃ saturated solution, then the obtained solution was collected and washed with a NaHCO₃ saturated solution. The aqueous and organic phases were collected and the aqueous phase was extracted using DCM. The combined organic phases were dehydrated using Na₂SO₄ and concentrated under vacuum. The crude presented itself as a brown oil.

Said oil was purified via flash column chromatography using silica as a stationary phase and a hexane/ AcOEt solution (9:1) as mobile phase and concentrated under vacuum. Finally, product **2** was isolated as a yellow oil (1.1905 g, 65,2% yield).

¹H NMR ¹H NMR (399 MHz, Chloroform-*d*) δ in ppm: 7.31 (t, *J* = 1.1 Hz, 1H, H3), 3.61 (m, *J* =, 2H, H17 and H18), 2.52 (td, *J* = 7.4, 1.2 Hz, 2H, H4), 1.61 (m, 2H, H5), 1.42 –1.21 (m, 22H, from H6 to H15), 1.06 (s, 3H, H20), 1.00 (s, 3H, H21), 0.87 (m, 3H, H16). **¹³C NMR** (100.6 MHz, CDCl₃) δ in ppm: 138.2 (C-2), 115.3 (C-3), 83.7 (C-1), 77.3 (C-17 and C-19), 32.1 (CH₂), 30.5 (C-18), 29.83 (CH₂), 29.81 (CH₂), 29.80 (CH₂), 29.76 (CH₂), 29.7 (CH₂), 29.5 (CH₂), 29.4 (CH₂), 29.3 (CH₂),

27.4 (C-5), 25.1 (C-4), 22.8 (CH₂), 22.6 (C-20/C-21), 22.3 (C-20/C-21), 14.3 (C-16).

Tert-butyl (S)-4-((R)-(6,6-dimethyl-2-tridecyl-4,8-dioxaspiro[2.5]oct-1-en-1-yl)(hydroxy)methyl)-2,2-dimethyloxazolidine-3-carboxylate **Synthesis**
(product 3)



Product **2** (253.9 mg, 0.7878 mmol) was put in a round bottom flask. Under a positive pressure of Argon and while stirring, dry HMPA (0.2656 ml, 1.526 mmol) and dry THF (3.45 ml) were added to the reaction vessel, which was then put in a Dewar vase at -55 C°. When the temperature stabilized, BuLi (2.5 M solution in hexane, 0.3123 ml, 0.78075 mmol) was added in a dropwise manner. After 30 minutes a solution obtained dissolving Garner's aldehyde (100.4 mg, 0.4379 mmol) in dry THF (0.7892 ml) was added, then the reaction was left stirring overnight at -55 C°.

The reaction crude has been quenched by addition of a NH₄Cl saturated solution (5 ml), then the reaction vessel was removed from the Dewar vase and it has been let reach room temperature under stirring. The crude has been now extracted with DCM, and the combined organic phases were desiccated with Na₂SO₄ and concentrated under vacuum to give a brown oil.

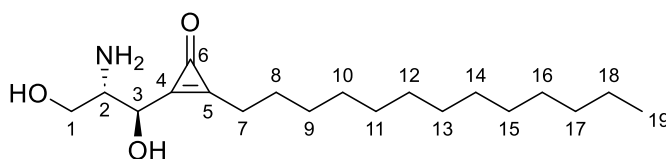
Said oil was purified via flash column chromatography (stationary phase silica gel, mobile phase hexane/AcOEt solution 9:1→8:2) and concentrated under vacuum. Product **3** was isolated as a yellow oil (153.9 mg, 63.7% yield).

α_D^{25} -8,4 (c 1.3, CHCl₃); **¹H NMR** (400 MHz, solvent CDCl₃, 50 C°) δ in ppm: 5.04-5.03 (m, 1H, H3), 4.16 (br s, 1H, H2), 4.00-3.99 (m, 2H, H1), 3.69-3.64 (m, 2H, H21 and H22), 3.56 (d, $J_{gem} = 11.0$ Hz, 2H, H21' and H22'), 2.47 (t, $J_{7-8} = 7.5$ Hz, 2H, H7), 1.65 – 1.57 (m, 6H, H26 and H27), 1.50 (s, 9H, H30, H31, H32), 1.37-1.26 (m, 22H, from H8 to H18), 1.06 (s, 3H, H23), 0.94 (s, 3H, H24), 0.88 (t, $J_{19-18} = 6.7$ Hz,

3H, H19). ^{13}C NMR δ in ppm (100.6 MHz, CDCl_3): 154.0 (C-28), 130.1 (C-5), 128.7 (C-4), 95.0 (C-25), 84.9 (C-6), 81.3 (C-29), 77.7 (C-20), 77.2 (C-22), 68.5 (C-3), 64.8 (C-1), 61.4 (C-2), 32.0 (CH_2), 30.4 (C-21), 29.82 (2CH_2), 29.79 (2CH_2), 29.78 (2CH_2), 29.76 (CH_2), 29.68 (CH_2), 29.55 (CH_2), 29.49 (CH_2), 29.40 (CH_2), 28.5 (3 C, C-30, C-31, C-32), 27.7 (C-8), 26.2 (2 C, C-26, C-27), 24.5 (C-7), 22.8 (CH_2), 22.6 (C-23), 22.2 (C-24), 14.3 (C-19).

2-((1R,2S)-2-amino-1,3-dihydroxypropyl)-3-tridecycycloprop-2-en-1-one

Synthesis (product 4)

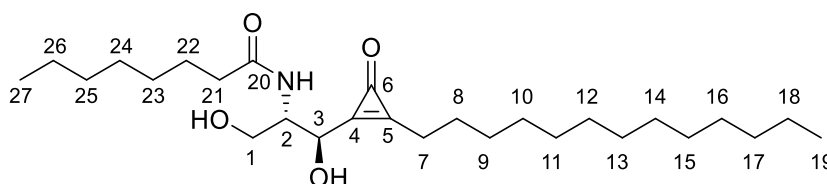


Product **3** (801.6 mg, 1.4527 mmol) was put in a round bottom flask and dissolved with distilled water (20.6 ml) and HCl (1M in AcOEt, 17.9259 mmol, 18 ml) and left under stirring at room temperature for 3 hours. After the reaction ended, the crude was evaporated under vacuum and dried using toluene.

The crude was purified via flash column chromatography (stationary phase silica gel 1:100, mobile phase DCM/MeOH/ NH_4OH solution 95:5:1 \rightarrow 90:10:1) and concentrated under vacuum. Product **4** was isolated as a white solid (342.5 mg, 72.4% yield).

$\alpha_D^{25} +1.6$ (c 1.1, MeOH); ^1H NMR (400 MHz, solvent CD_3OD) δ in ppm: 4.75 (br d, $J_{3-2} = 5.5$ Hz, $J_{3-7} = 1.0$ Hz, 1H, H3), 3.66 (dd, $J_{\text{gem}} = 11.0$ Hz, $J_{1-2} = 5.5$ Hz, 1H, H1), 3.61 (dd, $J_{\text{gem}} = 11.0$, $J_{1'-2} = 5.5$ Hz, 1H, H1'), 3.09 (q ap, $J_{2-1} = J_{2-3} = 5.5$ Hz, 1H, H2), 2.74 (td, $J_{7-8} = 7.2$ Hz, $J_{7-3} = 1.0$ Hz, 2H, H7), 1.75 (p, $J_{8-7} = J_{8-9} = 5.5$ Hz, 2H, H8), 1.46 – 1.26 (m, 20 H, from H9 to H18), 0.90 (t, $J_{19-18} = 7.0$ Hz, 3H, H19); ^{13}C NMR δ in ppm (100.6 MHz, CD_3OD): 162.8 (C-6), 162.0 (C-4), 161.2 (C-5), 71.3 (C-3), 63.6 (C-1), 57.6 (C-2), 33.1 (CH_2), 30.9 (CH_2), 30.82 (CH_2), 30.79 (CH_2), 30.76 (CH_2), 30.6 (CH_2), 30.5 (CH_2), 30.4 (CH_2), 30.3 (CH_2), 27.4 (C-8), 26.8 (C-7), 23.8 (CH_2), 14.5 (C-19).

***N*-((1*R*,2*S*)-1,3-dihydroxy-1-(3-oxo-2-tridecylcycloprop-1-en-1-yl)propan-2-yl)octanamide (PR280) (product 5)**



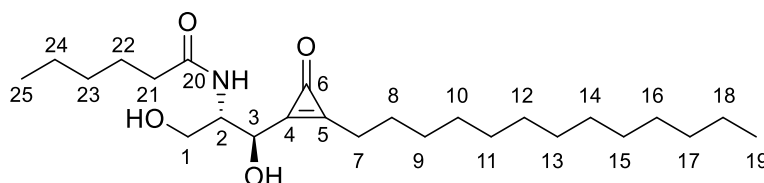
Octanoic acid (132 μ L, 0.83 mmol), EDC (160 mg, 0.83 mmol) and HOBt (114 mg, 0.84 mmol) were dissolved in dry CH_2Cl_2 (24 mL). The solution was stirred at room temperature for 45 min. The resulting mixture was added to a solution of product **4** (150 mg, 0.46 mmol) in dry CH_2Cl_2 (16 mL) and stirred at room temperature overnight.

After this time water was added, both phases were separated, and the aqueous phase was extracted with CH_2Cl_2 . The combined organic extracts were dried over anhydrous Na_2SO_4 , filtrated, and concentrated under vacuum to give a yellowish solid residue which was purified by flash column chromatography on silica gel (DCM/MeOH/ NH_4OH , 95:5:1). The resulting solid was crystallized with pentane and product **5** was obtained as a white solid (126 mg, 0.28 mmol, 60 % yield).

R_f = 0.09 DCM/MeOH/ NH_4OH (95:5:1); α_D^{25} -41.2 (c 0.5, CHCl_3); **M.p.** = 126-127 $^\circ\text{C}$;
 $^1\text{H NMR}$ δ in ppm (400 MHz, CDCl_3): 6.81 (d, $J_{\text{NH-2}}$ = 5.2 Hz, 1H, NH), 5.87 (d, $J_{\text{OH3-3}}$ = 5.2 Hz, 1H, OH-3), 4.82 (d, $J_{\text{3-OH3}}$ = 5.2 Hz, 1H, H-3), 4.2 (m, 1H, H-2), 4.02-3.98 (m, 2H, OH-1 and H-1), 3.94-3.89 (m, 1H, H-1'), 2.67 (t, J_{7-8} = 7.3 Hz, 2H, H-7), 2.29-2.17 (m, 2H, H-21), 1.75-1.68 (m, 2H, H-8), 1.59 (p, $J_{22-21} = J_{22-23} = 7.3$ Hz, 1H, H-22), 1.39-1.25 (m, 28H, from H-9 to H-18 and H-23 to H-26), 0.88 (t, $J_{19-18} = J_{27-26} = 6.5$ Hz, 6H, H-19 and H-27); **$^{13}\text{C NMR}$** δ in ppm (100.6 MHz, CDCl_3): 176.8 (C-20), 162.1 (C-5), 160.6 (C-4), 159.5 (C-6), 71.8 (C-3), 61.5 (C-1), 56.4 (C-2), 36.4 (C-21), 32.1 (CH_2), 31.8 (CH_2), 29.83 (CH_2), 29.80 (CH_2), 29.77 (CH_2), 29.6 (CH_2), 29.5 (CH_2), 29.4 (CH_2), 29.30 (CH_2), 29.28 (CH_2), 29.1 (CH_2), 26.6 (C-8), 26.3 (C-7), 25.8 (C-22), 22.79 (CH_2), 22.84 (CH_2), 22.76 (CH_2), 14.3 (CH_3), 14.21 (CH_3); **HRMS** (ESI+) for $[\text{M}+\text{H}]^+$ $\text{C}_{27}\text{H}_{50}\text{NO}_4^+$ (m/z): calculated: 452.37343, found: 452.37360; **FT-IR (ATR)** ν in cm^{-1} : 3307, 2955, 2920, 2871, 2851, 1838, 1647,

1577, 1546, 1465, 1418, 1377, 1329, 1293, 1264, 1243, 1207, 1122, 1073, 981, 944, 798, 721, 696, 654, 621, 537.

***N*-((1*R*,2*S*)-1,3-dihydroxy-1-(3-oxo-2-tridecylcycloprop-1-en-1-yl)propan-2-yl)hexanamide Synthesis (product 6)**



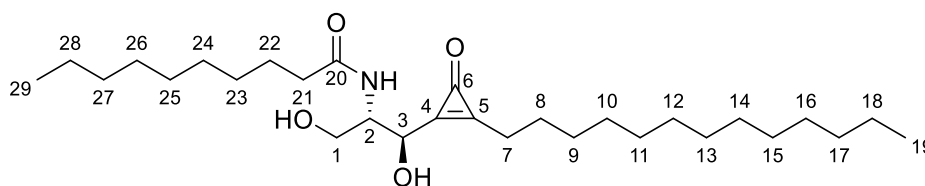
Hexanoic acid (21.5 μ L, 0.17 mmol), EDC (33.2 mg, 0.17 mmol) and HOBT (23.3 mg, 0.17 mmol) were dissolved in dry CH_2Cl_2 (4.9 mL). The solution was stirred at room temperature for 45 min. The resulting mixture was added to a solution of product **4** (50.9 mg, 0.16 mmol) in dry CH_2Cl_2 (5.4 mL) and stirred at room temperature overnight.

After this time water was added, both phases were separated, and the aqueous phase was extracted with CH_2Cl_2 . The combined organic extracts were dried over anhydrous Na_2SO_4 , filtrated, and concentrated under vacuum to give a yellowish solid residue which was purified by flash column chromatography on silica gel (DCM/MeOH/ NH_4OH , 96:4:1). The resulting solid was recrystallized with pentane and product **6** was obtained as a white solid (48.6 mg, 0.11 mmol, 73 % yield).

R_f = 0.37 DCM/MeOH/ NH_4OH (9:1:0.1); α_D^{25} -33.9 (c 0.6, CHCl_3); **M.p.** = 121-122 °C; **¹H NMR** δ in ppm (400 MHz, CDCl_3): 6.96 (d, $J_{\text{NH-2}}$ = 5.9 Hz, 1H, NH), 5.94 (d, $J_{\text{OH-3}}$ = 7.5 Hz, 1H, OH-3), 4.85-4.83 (m, 1H, H-3), 4.26-4.23 (m, 1H, OH-1), 4.22-4.17 (m, 1H, H-2), 3.99-3.93 (m, 1H, H-1), 3.90-3.84 (m, 1H, H-1') 2.66 (t, J_{7-8} = 7.4 Hz, 2H, H-7), 2.28-2.16 (m, 2H, H-21), 1.71 (p ap, $J_{8-7} = J_{8-9} = 7.2$ Hz, 2H, H-8), 1.59 (p, $J_{22-21} = J_{22-23} = 7.3$ Hz, 2H, H-22), 1.38-1.23 (m, 24 H, from H-9 to H-18, H-23 and H-24), 0.88 (t, $J = 7.0$ Hz, 3H, H-19/H-25), 0.88 (t, $J = 7.0$ Hz, 3H, H-19/H-25); **¹³C NMR** δ in ppm (100.6 MHz, CDCl_3): 176.5 (C-20), 162.2 (C-5), 160.6 (C-4), 159.5 (C-6), 72.1 (C-3), 61.5 (C-1), 56.5 (C-2), 36.3 (C-21), 32.1 (CH₂), 32.0

(CH₂), 29.82 (CH₂), 29.78 (2CH₂), 29.76 (CH₂), 29.6 (CH₂), 29.5 (CH₂), 29.4 (CH₂), 29.3 (CH₂), 26.6 (C-8), 26.2 (C-7), 25.4 (C-22), 22.8 (CH₂), 22.5 (CH₂), 14.3 (CH₃), 14.0(CH₃); **HRMS** (ESI+) for [M+H]⁺ C₂₅H₄₆NO₄⁺ (m/z): calculated: 424.34214, found: 424.34103; **FT-IR (ATR)** ν in cm⁻¹: 3303, 2953, 2851, 1838, 1645, 1577, 1547, 1466, 1457, 1417, 1376, 1326, 1289, 1254, 1217, 1120, 1071, 980, 952, 720, 695, 652, 620, 437.

***N*-((1*R*,2*S*)-1,3-dihydroxy-1-(3-oxo-2-tridecylcycloprop-1-en-1-yl)propan-2-yl)decanamide Synthesis (product 7)**



Decanoic acid (29.3 mg, 0.17 mmol), EDC (32.7 mg, 0.17 mmol) and HOBT (23.2 mg, 0.17 mmol) were dissolved in dry CH₂Cl₂ (4.9 mL). The solution was stirred at room temperature for 45 min. The resulting mixture was added to a solution of product **4** (50.9 mg, 0.16 mmol) in dry CH₂Cl₂ (5.4 mL) and stirred at room temperature overnight.

After this time water was added, both phases were separated, and the aqueous phase was extracted with CH₂Cl₂. The combined organic extracts were dried over anhydrous Na₂SO₄, filtrated, and concentrated under vacuum to give a yellowish solid residue which was purified by flash column chromatography on silica gel (DCM/MeOH/NH₄OH, 96:4:1). The resulting solid was recrystallized with pentane and product **7** was obtained as a white solid (49.6 mg, 0.10 mmol, 66 % yield).

R_f = 0.40 DCM/MeOH/NH₄OH (9:1:0.1); α_D^{25} -10.6 (c 0.4, CHCl₃/MeOH, 1:1); **M.p.** = 132-133 °C; **¹H NMR** δ in ppm (400 MHz, CDCl₃): 6.79 (d, J_{NH-2} = 5.6 Hz, 1H, NH), 5.84 (bs, 1H, OH-3), 4.82 (bs, 1H, H-3), 4.22-4.18 (m, 1H, H-2), 4.00 (dd, $J_{1-1'}$ = 11.3, J_{1-2} = 4.3 Hz, 1H, H-1), 3.90 (dd, $J_{1'-1}$ = 11.3, $J_{1'-2}$ = 5 Hz, 1H, H-1'), 2.67 (t, J_{7-8} = 7.5 Hz, 2H, H-7), 2.29-2.17 (m, 2H, H-21), 1.75-1.68 (m, 2H, H-8), 1.59 (p ap, J_{22-21} = J_{22-23} = 7.3 Hz, 2H, H-22), 1.38-1.26 (m, 32H, from H-9 to H-18 and H-23 to H-8), 0.88 (t, J_{19-18} = J_{28-29} = 6.5 Hz, 6H, H-19 and H-27); **¹³C NMR** δ in ppm (100.6

MHz, CDCl₃): 176.8 (C-20), 162.2 (C-5), 160.6 (C-4), 159.4 (C-6), 72.8 (C-3), 61.5 (C-1), 56.4 (C-2), 36.4 (C-21), 32.1 (CH₂), 32.0 (CH₂), 29.83 (CH₂), 29.80 (2CH₂), 29.78 (CH₂), 29.62 (CH₂), 29.60 (CH₂), 29.51 (CH₂), 29.49 (CH₂), 29.43 (2CH₂), 29.36 (CH₂), 29.3 (CH₂), 26.6 (C-8), 26.3 (C-7), 25.79 (C-22), 22.84 (CH₂), 22.81 (CH₂), 14.3 (CH₃), 14.2 (CH₃); **HRMS** (ESI+) for [M+H]⁺ C₂₉H₅₄NO₄⁺ (m/z): calculated: 480.40474, found: 480.40344; **FT-IR (ATR)** v in cm⁻¹: 3306, 2955, 2919, 2851, 1838, 1647, 1577, 1547, 1467, 1417, 1389, 1330, 1292, 1259, 1230, 1200, 1117, 1073, 981, 944, 721, 695, 654, 621, 537.

Bibliography and citations

- A.Ashkenazi, M. Viard, L. Unger, R. Blumenthal, Y. Shai; Sphingopeptides: dihydrosphingosine-based fusion against wild-type and enfuvirtide-resistant HIV-1, *FASEB Journal*, 26 (11), 4628 (2012);
- A.H. Merrill, *Biochemistry of Lipids, Lipoproteins and Membranes (Fifth Edition)*; Elsevier, 363-397(2008);
- B.T. Bikman, Y. Guan, G. Shui, M.M. Siddique, W.L. Holland, J.Y. Kim, G. Fabriàs, M.R. Wenk, S.A. Summers; Fenretinide prevents lipid-induced insulin resistance by blocking ceramide biosynthesis, *Journal of Biological Chemistry*, 287(21), 17426-17437 (2012);
- C. Bedia, G. Triola, J. Casas, A. Llebaria, G. Fabriàs; Analogs of the dihydroceramide desaturase inhibitor GT11 modified at the amide function: synthesis and biological activities; *Organic & Biomolecular Chemistry*, 3 (20), 3707-3712 (2005);
- C. Martí Torrell; Synthesis of potential dihydroceramide desaturase 1 inhibitors based on triazole motifs as a therapeutical target against cancer; Master thesis, Universitat Rovira i Virgili, SINTCARB group (2018) Lee, M., Lee, S.Y. & Bae, YS. Functional roles of sphingolipids in immunity and their implication in disease. *Exp Mol Med* **55**, 1110–1130 (2023);
- C.P. Reynolds, B.J. Maurer, R.N. Kolesnick; Ceramide synthesis and metabolism as a target for cancer therapy, *Cancer Letters*, 206 (2), 169-180 (2004);
- E. Bonandi, M.S. Christodoulou, G. Fumagalli, D. Perdicchia, G. Rastelli, D. Passarella; The 1,2,3-triazole ring as a bioisostere in medicinal chemistry, *Drug Discovery Today* 22 (10), 1572-1581 (2017);
- F. Wang, T. Luo, J. Hu, Y. Wang, H.S. Krishnan, P.V. Jog, S.K. Ganesh, G.K. Surya Prakash, G.A. Olah; Synthesis of *gem*-Difluorinated Cyclopropanes and Cyclopropenes: Trifluoromethyltrimethylsilane as a Difluorocarbene Source, *Angewandte Chemie International Edition*, 50 (31), 7153-7157 (2011);

- F.X. Conteras, G. Basañes, A. Alonso, A. Hermann, F.M. Goñi; Asymmetric addition of ceramides but not dihydroceramides Promotes transbilayer (Flip-Flop) Lipid Motion in Membranes, *Biophysical Journal*, 88(1), 348-359 (2005);
- G. Appendino, S. Bacchiega, A. Minassi, M.G. Cascio, L. DE Petrocellis, V. Di Marzo; The 1,2,3-Triazole Ring as a peptido-and olefinomimetic element: discovery of click vanilloids and cannabinoids, *Angewandte Chem* 119 (48), 9472 (2007);
- G. Triola, G. Fabriàs, A. Llebaria; Synthesis of a Cyclopropene Analogue of Ceramide, a Potent Inhibitor of Dihydroceramide Desaturase. *Angewandte Chemie (International ed. In English)*, 40 (10), 1960-1962 (2001);
- H. Tokuyama, M. Isaka, E. Nakamura, R. Ando, Y. Morinaka; Synthesis and biological activities of cyclopropenone antibiotic penitricin and congeners, *The Journal of antibiotics*, 45 (7), 1148-1154 (1992);
- J. Jumper et al; AlphaFold 2. Fourteenth Critical Assessment of Techniques for Protein Structure Prediction (2020);
- J. Sasa, H. Zhangxu, D. Yuanbing, J. Gang, W. Kaiyue, Y. Feifei, Z. Jingyu; An Overview of cyclopropenone derivate as promising bioactive molecules, *Bioorganic & Medicinal Chemistry Letters*, 129845 (2024);
- L. A. Peterson; Reactive Metabolites in the Biotransformation of Molecules Containing a Furan Ring; *Chemical Research in Toxicology*, 26 (1), 6-25 (2013);
- L. Camacho, F. Simbari, M. Garrido, J.L. Abad, J. Casas, A. Delgado, G. Fabriàs; 3-Deoxy-3,4-dehydro analogs of XM462. Preparation and activity on sphingolipid metabolism and cell fate; *Bioorganic & Medicinal Chemistry*, 20 (10), 3173-3179 (2012);
- L.M. Bertoline, A.N. Lima, J.E. Krieger, S.K. Teixeira; Before and after AlphaFold2: An overview of protein structure prediction; *Frontiers in Bioinformatics*, 3, 1120370 (2013);

- L.M. Obeid, C.M. Linardic, L.A. Karolak, Y.A. Hannun, Programmed Cell Death Induced by Ceramide. *Science*, 259 (5102), 1769–1771 (1993);
- L. Wong, S. Tan, Y. Lam, A.J. Melendez; Synthesis and evaluation of sphingosine analogues as inhibitors of sphingosine kinases, *Journal of Medicinal Chemistry*, 52 (12), 3618-3626 (2009);
- M. Lee, S.Y. Lee, Y.S. Bae; Functional roles of sphingolipids in immunity and their implication in disease. *Exp Mol Med* **55**, 1110–1130 (2023).
- M.M. Siddique, Y. Li, B. Chaurasia, V.A. Kaddai, S.A. Summers; Dihydroceramides: From bit Players to Lead Actors, *Journal of Biological Chemistry*, 290 (25), 15371-15379 (2015);
- M. Munoz-Olaya, X. Matabosh, C Bedia, M. Egido-Gabás, J. Casas, A. Llebaria, A. Delgado, G. Fabriàs; Synthesis and biological activity of a novel inhibitor of dihydroceramide desaturase; *ChemMedChem: Chemistry Enabling Drug Discovery*, 3 (6), 946-953 (2008);
- M. Nakamura, I. Hiroyuki, E. Nakamura; Cyclopropanone acetals synthesis and reactions, *Chemical reviews*, 103 (4), 1295-1326 (2003);
- M. Passiniemi, A.M. Koskinen; Garner's aldehyde as a versatile intermediate in the synthesis of enantiopure natural products, *Beilstein journal of organic chemistry*, 9 (1), 2641-2659 (2013);
- O. Cuvillier, G. Pirianov, B. Kleuser, P.G. Vanek, O.A. Coso, J.S. Gutkind, S. Spiegel, Suppression of ceramide-mediated programmed cell death by sphingosine-1-phosphate; *Nature*, 381 (6585), 800-803 (1996);
- O.K. Karjalainen, A.M. Koskinen; Diastereoselective synthesis of vicinal amino alcohols, *Organic & Biomolecular Chemistry*, 10 (22), 4311-4326 (2012);
- P. Garner, J.M. Park; The synthesis and configurational stability of differentially protected .beta.-hydroxy-.alpha.-amino aldehydes, *The Journal of Organic Chemistry*, 52 (12), 2361-2364 (1987);
- P. Rivero Prieto, PhD student, SINTCARB group;

- P. Rivero, V. Ivanova, X. Barril, M. Casampere, J. Casas, G. Fabriàs, Y. Díaz, M.I. Matheu; Targeting dihydroceramide desaturase 1 (Des1): Syntheses of ceramide analogues with a rigid scaffold, inhibitory assays, and AlphaFold2-assisted structural insights reveal cyclopropenone PR280 as a potent inhibitor, *Bioorganic Chemistry*, 145, 107233 (2024).
- S. Grassi, L. Mauri, S. Prioni, L. Cabitta, S. Sonnino, A. Prinetti, P. Giussani; Sphingosine 1-phosphate receptors and metabolic enzymes as druggable targets for brain diseases; *Frontiers in Pharmacology*, 10, 807 (2019);
- S. Pyne, D.R. Adams, N.J. Pyne, Sphingosine 1-phosphate and sphingosine kinases in health and disease: Recent advances; *Progress in Lipid research*, 62, 93-106 (2016);
- S. Rodriguez-Cuenca, N. Barbarroja, A. Vidal-Puig; Dihydroceramide desaturase 1, the gatekeeper of ceramide induced lipotoxicity, *Biochimica et Biophysica Acta (BBA) – Molecular and Cell Biology of Lipids* 1851 (1), 40-50 (2015);
- W.H. Sikorski, H.J. Reich; The regioselectivity of addition of organolithium reagents to enones and enals: the role of HMPA, *Journal of the American Chemical Society*, 123 (27), 6527-6535 (2001);
- W. Zheng, J. Kollmeyer, H. Symolon, A. Momin, E. Munter, E. Wang, S. Kelly, J.C. Allegood, Y. Liu, O. Peng, H. Ramaraju, M. Cameron Sullards, M. Cabot, A.H. Merrill; Ceramides and other bioactive sphingolipid backbones in health and disease: Lipidomic analysis, metabolism and roles in membrane structure, dynamics, signaling and autophagy; *Biochimica et Biophysica Acta (BBA) – Biomembranes*, 1758 (12), 1864-1884 (2006);
- X. Liang, J. Andersch, M. Bols; Garner's aldehyde, *Journal of Chemical Society, Perkin Transactions 1*, (18), 2136-2157 (2001);
- Z.-L. Cheng, Q.-Y. Chen; Difluorocarbene Chemistry: A Simple Transformation of 3,3-gem-Difluorocyclopropenes to Cyclopropenones, *Chinese Journal of Chemistry*, 24 (9), 1219-1224 (2006).

Sitography

AlphaFold 2 Protein Structures Database, <https://alphafold.ebi.ac.uk/entry/O15121>